Supporting Information

Garrity et al. 10.1073/pnas.0913280107

SI Materials and Methods

Plasmids, Strains, and Cell Growth. When present individually, fusion proteins were produced from pBR322-derived plasmids under the control of the arabinose-inducible promoter pBAD. In experiments in which New1-CFP-3xHA was produced together with NM-YFP, New1-CFP-3xHA was produced under the control of an IPTG-inducible promoter from either a pACYC184-derived plasmid or a chromosomally integrated construct.

Extract Seeding and Filter Retention Assay. The cellulose acetate membrane was soaked in PBS followed by assembly into a 96-well dot-blotting vacuum manifold. To equilibrate the membrane, 200 μL PBS containing 2% SDS was filtered through the membrane. A 5-μL quantity of the thawed samples was then added to 100 μL PBS containing 2% SDS, and the mixture was filtered through the membrane. Samples on the membrane were then washed twice with 200 μL PBS containing 2% SDS and twice with 200 μL PBS. After removal from the vacuum manifold, the membrane was probed with anti-Sup35 yS-20 to detect immobilized protein.

Bacteria and Yeast Fusions. Partial lysis of bacteria during preparation of the protoplasts liberates some plasmid DNA that can mediate transformation of the recipient yeast spheroplasts without protoplast fusion. To control for URA^+ transformants that arose from transformation with liberated plasmid DNA (as opposed to URA^+ transformants that arose from direct protoplast fusion), the bacterial protoplast preparations were pelleted at 3,000 × *g* and the supernatants used to transform the recipient yeast spheroplasts. Quantification of the efficiencies of these control (supernatant-only) transformations indicated that an average of 11.5% (range, 5–21%) of the total transformants observed with the protoplast mixtures arose due to the uptake of liberated DNA. [PSI^+] yeast cells were not observed among these transformants.

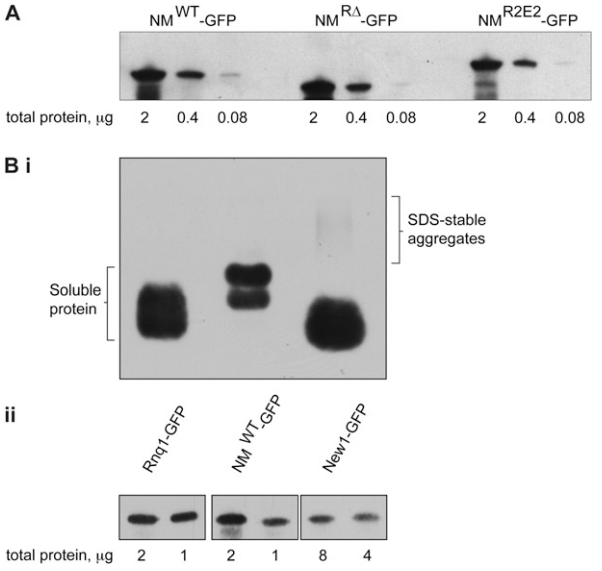

Fig. S1. Levels of GFP-fusion constructs in *E. coli*. (*A*) Western blot (anti-GFP) analysis of *E. coli* cell extracts containing NM^{WT}-GFP, $NM^{R\Delta}$-GFP, or NM^{R2E2}-GFP. (*B*) (*i*) SDD-AGE analysis of *E. coli* cell extracts containing Rnq1-GFP, NM^{WT}-GFP, or New1-GFP. In the case of Rnq1-GFP and NM^{WT}-GFP, the extracts were prepared 5 h after induction of fusion protein synthesis, whereas in the case of New1-GFP, the extract was prepared 1 h after induction of fusion protein synthesis, at which times the intracellular level of the New1-GFP fusion protein was significantly lower than the levels of the other fusion proteins. To compensate for this difference in fusion protein levels, 20-fold more total protein was loaded for extract containing New1-GFP. Because the blot reveals a faint higher-molecular-weight smear indicative of SDS-stable aggregates only in the case of the New1-GFP fusion protein, we infer that this fusion protein begins to undergo conversion to the prion form even when its intracellular concentration is substantially lower than concentrations of the other two fusion proteins that do not promote detectable conversion to the prion form. We note that by 5 h after induction of fusion protein synthesis, the New1-GFP fusion protein has accumulated to significantly higher levels than have the other two fusion proteins, which is potentially due to the presence of the New1-GFP fusion protein in the amyloid form, which may lead to a decrease in the rate of turnover of this protein in the cell. (B) (*ii*) Western blot analysis of cell extracts from *i* revealed the New1-GFP level to be approximately 8-fold less than the level of NM-GFP and greater than 8-fold less than the level of Rnq1-GFP. Blots were probed with anti-GFP antibody.

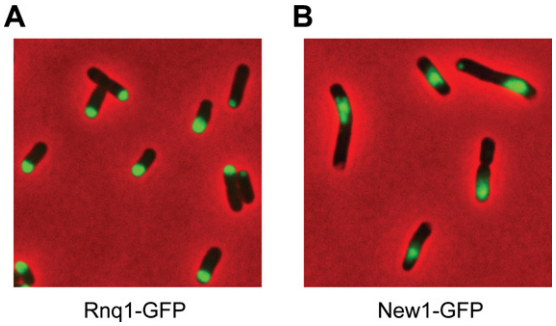

Fig. S2. Behavior of New1- and Rnq1-GFP fusion proteins in *E. coli* cells. Fluorescence images of cells containing either Rnq1-GFP (*A*) or New1-GFP (*B*) fusion protein. Cells were transformed with plasmids encoding each fusion protein under the control of an inducible promoter. Images show cells examined after the induction of fusion protein synthesis for 5.5 h.

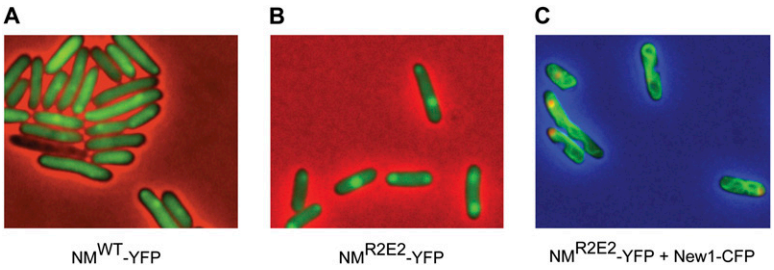

Fig. S3. Behavior of NM-YFP fusion proteins in *E. coli*. (*A* and *B*) Fluorescence images of cells containing the indicated NM-YFP fusion protein. Cells were transformed with plasmids encoding each fusion protein under the control of an inducible promoter. Images show cells examined after induction of fusion protein synthesis for 5 h. No twisted ribbons were observed for cells producing NM^{WT}-YFP (256 cells examined) or NM^{R2E2}-YFP (347 cells examined). (*C*) Fluorescence image of cells containing New1-CFP (colored red) together with NM^{R2E2}-YFP (colored green), 5.5 h after induction of NM^{R2E2}-YFP fusion protein synthesis.

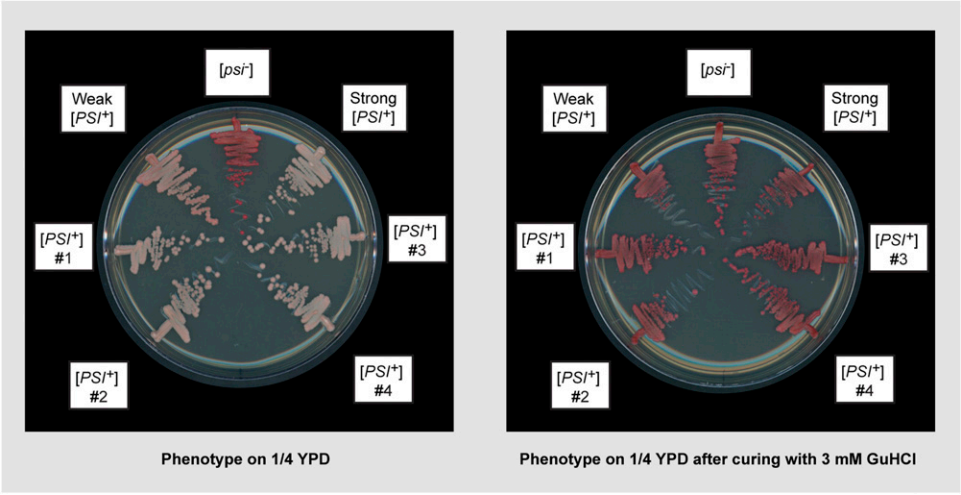

Fig. S4. Phenotypes of [*PSI*$^+$] yeast strains that arose via fusion with *E. coli* protoplasts. Comparison of phenotypes of four representative [*PSI*$^+$] yeast strains that were obtained via fusion with *E. coli* protoplasts (labeled [*PSI*$^+$] #1–4) with those of a strong [*PSI*$^+$] (SG862), a weak [*PSI*$^+$] (SG863), and a [*psi*$^-$] (SG775) control strain on 1/4 YPD both before (*Left*) and after (*Right*) curing via passage on medium containing 3 mM GuHCl. Additional strain details are given in Table S1.

A

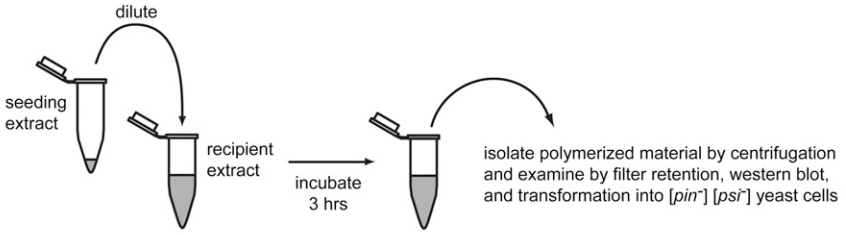

B

Polymerization Reaction		Filter Retention	Protein Transformation
Seed Extract*	Recipient Extract		% [*PSI*⁺]; ([*PSI*⁺] / Total)
S. cerevisiae [*psi*⁻]	*E. coli* NM^{wt}-GFP		1%; (10 / 1000)
S. cerevisiae strong [*PSI*⁺]	*E. coli* NM^{wt}-GFP		27%; (161 / 600)
E. coli NM^{wt}-YFP + New1-CFP	*E. coli* NM^{wt}-GFP		23%; (171 / 752)
E. coli NM^{wt}-YFP	*E. coli* NM^{wt}-GFP		0.4%; (2 / 520)
S. cerevisiae [*psi*⁻]	*E. coli* GFP only		0%; (0 / 688)
S. cerevisiae strong [*PSI*⁺]	*E. coli* GFP only		0%; (0 / 664)
E. coli NM^{wt}-YFP + New1-CFP	*E. coli* GFP only		0.1%; (1 / 776)
E. coli NM^{wt}-YFP	*E. coli* GFP only		0%; (0 / 392)

C

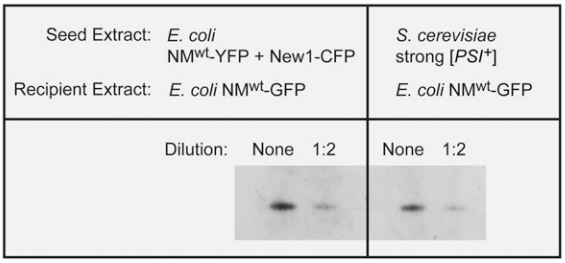

Fig. S5. Comparison of infectivity of NM-GFP polymerized in vitro using either *S. cerevisiae*– or *E. coli*–derived material as seed. (*A*) Illustration of experimental protocol, analogous to experiment in Fig. 3*A* in main text. (*B*) Indicated *E. coli* and *S. cerevisiae* seed extracts were added to recipient *E. coli* extracts (100 μL of 2 mg/mL total protein) containing either NM^{wt}-GFP or GFP alone. These seeded polymerization reactions were then incubated at RT without agitation. After 3 h, polymerized material was harvested by centrifugation at 10,000 × *g* for 15 min at 4 °C, washed in 500 μL STC buffer, and centrifuged again at 10,000 × *g* for 15 min at 4 °C. Pelleted material was resuspended in 500 μL STC buffer. A 5-μL quantity of this resuspended material was treated with 2% SDS at RT and analyzed by filter retention (protocol described in *Materials and Methods* in main text). The detected membrane, probed with anti–Sup35 yS-20 (Santa Cruz Biotechnology), shows polymerized, SDS-stable aggregates that were retained. A second aliquot of the material resuspended after centrifugation was sonicated briefly (Sonics Vibracell Microtip sonicator, 25% amplitude, pulsed 1 s "on" and 3 s "off" for a total of 25 s of "on" time), and transformed into [*pin*⁻] [*psi*⁻] yeast cells (protocol described in *Materials and Methods* in main text). Frequency of [*PSI*⁺] observed in these transformations (as percentage of total transformants) is shown. Consistent with what has been observed previously when assaying the infectivity of in vitro polymerized material (1, 2), we found that the sonication step enhanced infectivity of in vitro polymerized NM-GFP. *Note: To obtain comparable amounts of polymerized NM-GFP after 3 h in reactions seeded with material from *S. cerevisiae* [*PSI*⁺] and from *E. coli* containing NM-YFP and New1-CFP, different amounts of *S. cerevisiae* (5 μL of 0.18 mg/mL) and *E. coli* (5 μL of 1 mg/mL) seed extracts were used (control *S. cerevisiae* and *E. coli* seed extracts were used at these same concentrations). (*C*) Polymerized material harvested by centrifugation from indicated reactions was analyzed by SDS/PAGE and Western blot. Blot, probed with anti–Sup35 yS-20, shows that comparable levels of material were present in these samples.

1. King CY, Diaz-Avalos R (2004) Protein-only transmission of three yeast prion strains. *Nature* 428:319–323.
2. Tanaka M, Weissman JS (2006) An efficient protein transformation protocol for introducing prions into yeast. *Methods Enzymol* 412:185–200.

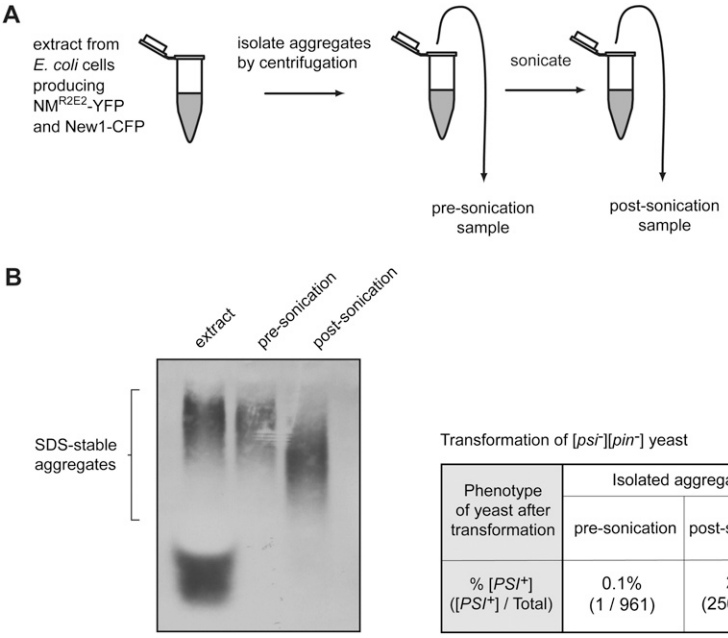

Transformation of [*psi*$^-$][*pin*$^-$] yeast

Phenotype of yeast after transformation	Isolated aggregates	
	pre-sonication	post-sonication
% [*PSI*$^+$] ([*PSI*$^+$] / Total)	0.1% (1 / 961)	28% (256 / 912)

Fig. S6. Sonication of NM-YFP amyloid aggregates isolated from *E. coli* cells increases infectivity and decreases apparent polymer size. (*A*) A 500-μL quantity of 1 mg/mL extract of *E. coli* cells producing NM^{R2E2}-YFP and New1-CFP (prepared as described in *Materials and Methods* in main text) was centrifuged at 10,000 × *g* for 15 min at 4 °C, washed in 500 μL STC buffer, and centrifuged again at 10,000 × *g* for 15 min at 4 °C to isolate amyloid aggregates present in extract. The resulting pellet was resuspended in STC buffer, and samples were removed for SDD-AGE analysis and protein transformation. The remainder of the resuspended pellet was then sonicated (Sonics Vibracell Microtip sonicator, 25% amplitude, pulsed 1 s "on" and 3 s "off" for a total of 25 s of "on" time), and samples were similarly removed for SDD-AGE analysis and protein transformation. (*B*) (*Left*) SDD-AGE and Western blot analysis (probed with anti-Sup35 yS-20) showing isolation of amyloid aggregates via centrifugation (compare lanes 1 and 2) and subsequent decrease in average size of isolated amyloid material postsonication (compare lanes 2 and 3). (*Right*) protein transformations, performed as described in *Materials and Methods* in main text, using material isolated via centrifugation both pre- and postsonication.

Table S1. Plasmids and strains used in this study

Strain/plasmid	Genotype or relevant characteristics	Source/Reference
Plasmid		
p316CUP1-3S GFP.SG	*URA3* P_{CUP1}-*SUP35NM*^{WT}-*GFP* pMB1 *ori bla CEN6*; pRS316 producing Sup35NM (residues 1–253) fused to GFP under the control of the CUP1 promoter.	(1)
pSG153	*bla* P_{BAD} *sup35NM*^{WT}-*gfp* pBR322 *ori*; produces Sup35NM^{WT} (Sup35 residues 1–253) fused to GFP	This study
pSG154	*bla* P_{BAD} *sup35NM*$^{R\Delta}$-*gfp* pBR322 *ori*; produces Sup35NM$^{R\Delta}$ (Sup35 residues 1–253 with deletion of oligopeptide repeats 2–5) fused to GFP	Plasmid, this study; Sup35 variant (1)
pSG155	*bla* P_{BAD} *sup35NM*^{R2E2}-*gfp* pBR322 *ori*; produces Sup35NM^{R2E2} (Sup35 residues 1–253 with oligopeptide repeat 2 expanded 2 additional times) fused to GFP	Plasmid, this study; Sup35 variant (1)
pSG241	*bla* P_{BAD} *sup35NM*^{WT}-*yfp* pBR322 *ori*; produces Sup35NM^{WT} (residues 1–253) fused to YFP	This study
pSG242	*bla* P_{BAD} *sup35NM*$^{R\Delta}$-*yfp* pBR322 *ori*; produces Sup35NM$^{R\Delta}$ (Sup35 residues 1–253 with deletion of oligopeptide repeats 2–5) fused to YFP	Plasmid, this study; Sup35 variant (1)
pSG243	*bla* P_{BAD} *sup35NM*^{R2E2}-*yfp* pBR322 *ori*; produces Sup35NM^{R2E2} (Sup35 residues 1–253 with oligopeptide repeat 2 expanded 2 additional times) fused to YFP	Plasmid, this study; Sup35 variant (1)
pSG378	*URA3* pACYC184 *ori cat CEN6*; shuttle vector pRS316 modified to contain pBR322-compatible origin and chloramphenicol resistance	This study
pVS20	*bla* P_{BAD} *rnq1-gfp* pBR322 *ori*; produces Rnq1 (full length) fused to GFP	This study
pVS23	*bla* P_{BAD} *new1*$_{50–100}$-*gfp* pBR322 *ori*; produces New1 (residues 50–100) fused to GFP	This study
pVS30	*cat* P_{lacUV5} *new1*$_{50–100}$-*cfp-3xha* pACYC184 *ori*; produces New1 (residues 50–100) fused to CFP and 3 HA tags	This study
Strain (*Escherichia coli*)		
BW27785	Δ(*araB-araD*)*567* Δ*lacZ4787*(::rrnB-3) LAM- Δ(*araH-araF*)*570*(::FRT) ΔaraEp-532::FRT ϕ(P_{cp18}-*araE534*) Δ(*rhaB-rhaD*)*568 hsdR514*	(2)
SG811	BW27785 attB::*ahp laclq* P_{tac} *new1*$_{50–100}$-*cfp-3xha*; produces New1 (residues 50–100) fused to CFP and 3 HA tags from a chromosomal construct integrated at lambda attachment site.	Plasmid, this study; construction method (3)
Strain (*Saccharomyces cerevisiae*)		
SG775	YJW187 [*pin*$^-$]; derived by serial passage on YPD with 3 mM GuHCl; phenotypically [*pin*$^-$] [*psi*$^-$]	This study
SG823	YJW187 [*PSI*$^+$] containing p316CUP1-3SGFP.SG; derived by transient overproduction of NM^{WT}-GFP on SD-URA plates and subsequent selection on SD-URA-ADE plates. Checked for curing by 3 mM GuHCl; phenotypically strong [*PSI*$^+$]	This study
SG824	YJW187 [*PSI*$^+$] containing p316CUP1-3SGFP.SG; derived by transient overproduction of NM^{WT}-GFP on SD-URA plates and subsequent selection on SD-URA-ADE plates; checked for curing by 3 mM GuHCl; phenotypically weak [*PSI*$^+$]	This study
SG825	YJW187 containing p316CUP1-3SGFP.SG; phenotypically [*psi*$^-$]	This study
SG848	SG775 [*PSI*$^+$] (#1); derived by protoplast fusion with *E. coli*; phenotypically strong [*PSI*$^+$]	This study
SG849	SG775 [*PSI*$^+$] (#2); derived by protoplast fusion with *E. coli*; phenotypically strong [*PSI*$^+$]	This study
SG850	SG775 [*PSI*$^+$] (#3); derived by protoplast fusion with *E. coli*; phenotypically strong [*PSI*$^+$]	This study
SG852	SG775 [*PSI*$^+$] (#4); derived by protoplast fusion with *E. coli*; phenotypically strong [*PSI*$^+$]	This study
SG861	YJW187 [*PSI*$^+$]; derived by losing plasmid from SG824 by repeated restreaking on YPD plates; phenotypically weak [*PSI*$^+$]	This study
SG862	SG775 [*PSI*$^+$]; derived by protein transformation with material from YJW96; phenotypically strong [*PSI*$^+$]	This study
SG863	SG775 [*PSI*$^+$]; derived by protein transformation with material from SG861; phenotypically weak [*PSI*$^+$]	This study
YJW96	74D-694 *MATa ade1-14*(UGA) *his3 leu2 trp1 ura3* [*PSI*$^+$]; phenotypically strong [*PSI*$^+$]	(4)
YJW187	74D-694 *MATa ade1-14*(UGA) *his3 leu2 trp1 ura3* [*psi*$^-$] [*PIN*$^+$]	(4)

1. Liu JJ, Lindquist S (1999) Oligopeptide-repeat expansions modulate 'protein-only' inheritance in yeast. *Nature* 400:573–576.
2. Khlebnikov A, Datsenko KA, Skaug T, Wanner BL, Keasling JD (2001) Homogeneous expression of the P(BAD) promoter in Escherichia coli by constitutive expression of the low-affinity high-capacity AraE transporter. *Microbiology* 147:3241–3247.
3. Haldimann A, Wanner BL (2001) Conditional-replication, integration, excision, and retrieval plasmid-host systems for gene structure-function studies of bacteria. *J Bacteriol* 183: 6384–6393.
4. Tanaka M, Chien P, Naber N, Cooke R, Weissman JS (2004) Conformational variations in an infectious protein determine prion strain differences. *Nature* 428:323–328.